Spatiotemporal-controllable ROS-responsive Camptothecin Nano-bomb for Chemo/photo/immunotherapy in Triple-Negative Breast Cancer

Wenjie Xu[1,3,#], Zhaokui Zeng[2,#], Yucheng Tang[1,3], Jingjing Tian[2], Xinyan Hao[1,3], Pengcheng Sun[1,3], Yanjin Peng[1,3], Tian Tian[2], Daxiong Xiang[1,3], Rongrong Wang[4,*], Chuanpin Chen[2,*], Junyong Wu[1,3,5,*]

1 Department of Pharmacy, The Second Xiangya Hospital, Central South University, 410011, Changsha, China

2 Department of Pharmacy, Xiangya School of Pharmaceutical Sciences, Central South University, Changsha 410000, China

3 Hunan Provincial Engineering Research Centre of Translational Medicine and Innovative Drug, 410011, Changsha, China

4 Hunan Institute of Drug Inspection, 60 Bayi Road, Changsha, Hunan 410001, China

5 Hunan Key Laboratory of Tumor Models and Individualized Medicine, The Second Xiangya Hospital, Central South University, 410011, Changsha, China

*Corresponding Authors: Rongrong Wang: 273199683@qq.com; Chuanpin Chen: ccpin2000@hotmail.com; Junyong Wu: wujunyong@csu.edu.cn.

# Wenjie Xu and Zhaokui Zeng contributed equally to this work.

Synthesis and Characterization of TK-CPT

To prepare ROS-responsive CTF, we first synthesized the ROS-sensitive TK moiety. The structure of TK was confirmed by proton nuclear magnetic resonance (1H NMR) spectroscopy, with the results shown in Figure S2. The 1H NMR (400 MHz, DMSO-d6) spectrum displayed signals at δ 12.29 (s, 2H), 2.74 (t, J = 7.2 Hz, 4H), 2.54-2.48 (t, 4H), and 1.53 (s, 6H). Due to the symmetrical nature of TK, the integration for protons at positions 1, 2, 3, and 4 was doubled, with an additional proton overlapping with the solvent peak at position 3. These results confirm the successful synthesis of TK. Using EDC and DMAP as catalysts, the carboxyl group on one end of TK reacted with the hydroxyl group of CPT under anhydrous conditions to form an esterification product. The crude product was purified by silica gel column chromatography. The resulting pure compound was characterized by 1H NMR spectroscopy, as shown in Figure S4.^{1}H NMR (400 MHz, DMSO-d6) δ 12.22 (s, 1H), 8.71 (s, 1H), 8.14 (dd, J = 8.4, 3.9 Hz, 2H), 7.88 (ddd, J = 8.5, 6.9, 1.4 Hz, 1H), 7.72 (t, J = 7.8 Hz, 1H), 7.25 (s, 1H), 5.51 (s, 2H), 5.39 – 5.22 (m, 2H), 2.70 (td, J = 7.2, 1.9 Hz, 2H), 2.42 (t, J = 7.1 Hz, 2H), 2.22 – 2.10 (m, 2H), 1.58 (s, 3H), 1.51 (s, 3H), 0.94 (t, J = 7.4 Hz, 3H). The mass spectrum is shown in Figure S5. The mass spectrum revealed a $[M+H]^+$ peak with a measured value of 583.1776 (theoretical value: 583.1501). These results confirm the successful synthesis of the ROS-responsive TK-CPT.

Synthesis and Characterization of CTF

TK-CPT and FUDR were mixed in a 1:1 molar ratio, and the carboxyl group of TK-CPT reacted with the hydroxyl group of FUDR to form the final target prodrug, CPT-TK-FUDR. The 1H NMR spectrum of CTF is shown in Figure S7，^{1}H NMR (500 MHz, DMSO-d_6) δ 11.85 (s, 1H), 9.04 (s, 1H), 8.70 (s, 1H), 8.12 (ddd, *J* = 8.1, 6.3, 1.2 Hz, 2H), 7.89–7.83 (m, 2H), 7.74–7.69 (m, 1H), 7.24 (s, 1H), 7.13 (d, *J* = 2.5 Hz, 1H), 6.99 (dd, *J* = 8.3, 2.5 Hz, 1H), 6.68 (d, *J* = 8.3 Hz, 1H), 6.10 (td, *J* = 6.7, 1.7 Hz, 1H), 5.50 (s, 1H), 5.40 (d, *J* = 4.4 Hz, 1H), 5.34 – 5.28 (m, 2H), 4.22 (tt, *J* = 6.2, 3.1 Hz, 1H), 4.21 – 4.14 (m, 2H), 3.87 (dt, *J* = 5.6, 4.1 Hz, 1H), 3.52 (tdd, *J* = 7.1, 4.4, 2.9 Hz, 1H), 2.73 (td, *J* = 7.1, 3.4 Hz, 2H), 2.66 (td, *J* = 7.0, 3.9 Hz, 1H), 2.56 (q, *J* = 7.1 Hz, 2H), 2.20 – 2.13 (m, 2H), 2.00 (dp, *J* = 12.9, 6.3 Hz, 1H), 1.50 (s, 2H), 1.34 (s, 9H), 1.23 (s, 10H), 0.90 – 0.77 (m, 3H).

The mass spectrum, shown in Figure S8, displayed a $[M+H]^+$ peak with a measured value of

811.2121 (theoretical value: 811.2051). These results confirm the successful synthesis of CTF.

Synthesis and Characterization of IR-780-NH_2

To successfully obtain the amphiphilic polymer HA-IR-780, 4-aminothiophenol was first reacted with IR-780 in a substitution reaction to yield the intermediate product IR-780-NH2. The 1H NMR spectrum of IR-780-NH2 is shown in Figure 2-11. ^{1}H NMR(500 MHz, Chloroform-d) δ 6.13 (d, J = 14.1 Hz, 2H), 4.01 (t, J = 7.4 Hz, 4H), 1.82 (q, J = 7.3 Hz, 5H), 1.49 (s, 12H), 0.98 (t, J = 7.4 Hz, 7H), 8.70 (d, J = 14.1 Hz, 2H), 7.32 – 7.23 (m, 4H), 7.14 (t, J = 7.5 Hz, 2H), 7.04 (d, J = 8.0 Hz, 2H), 6.97 – 6.93 (m, 2H), 6.59 (d, J = 8.6 Hz, 2H), 2.64 (t, J = 6.2 Hz, 4H), 1.93 (t, J = 6.1 Hz, 2H).This result demonstrates the successful synthesis of IR-780-NH_2.

Synthesis and Characterization of HA-IR780

Building upon the synthesis of IR780NH_2, the terminal amino group reacted with the carboxyl group at the active center of HA using EDC/NHS catalysis to form HAIR780. A sample of 1 mg HA-IR-780 was mixed and ground uniformly with 100 mg of dried potassium bromide powder, then pressed into pellets in a mold. Spectral scanning was performed using a Fourier-transform infrared (FTIR) spectrometer. As shown in Figure S12, the absorption peak at 3427 cm^{-1} corresponds to the characteristic hydroxyl group of HA. The IR780 absorption peaks predominantly appear in the fingerprint region of 400-1500 cm^{-1}. Additionally, a new peak at 1728 cm^{-1} appears for HAIR-780, corresponding to the carbonyl group's characteristic absorption peak. The original characteristic peaks of HA and IR780 are also retained, indicating successful grafting of IR780 onto HA.

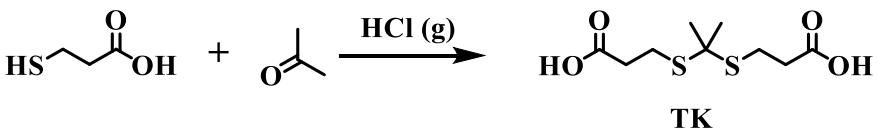

TK

Figure S1. The synthetic route of TK.

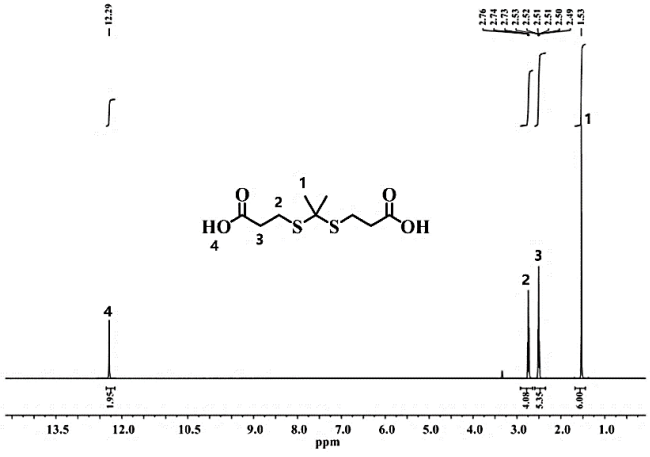

Figure S2. The ^{1}H NMR spectrum of TK in DMSO.

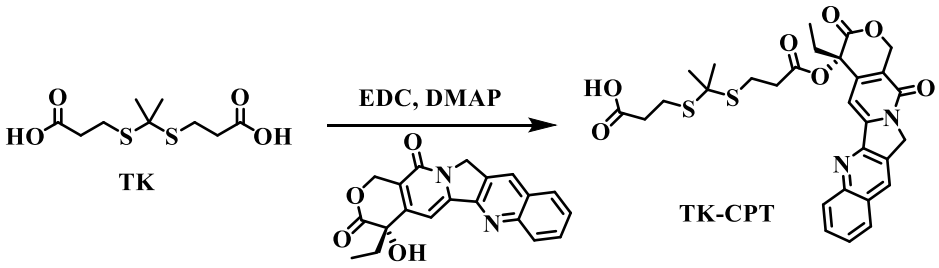

Figure S3. The synthetic route of TK-CPT.

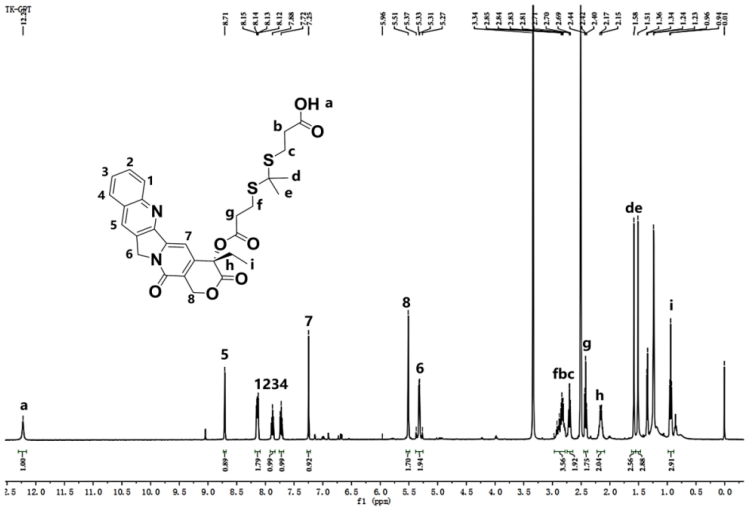

Figure S4. The ^{1}H NMR spectrum of TK-CPT in DMSO.

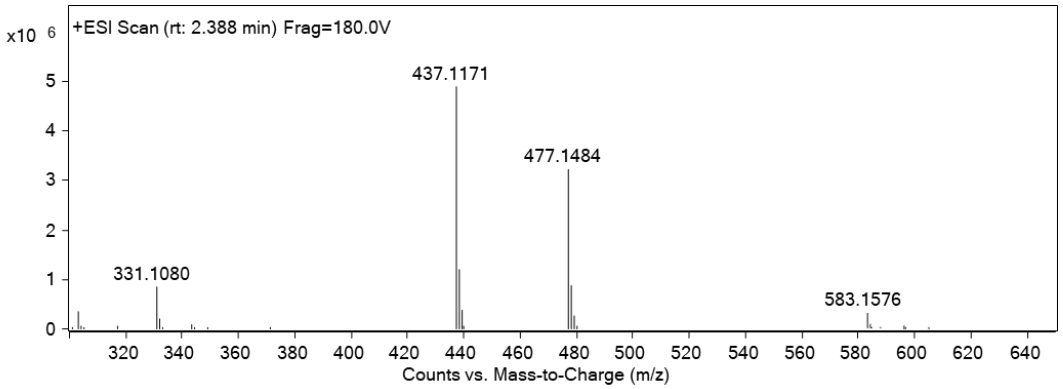

Figure S5. The mass spectrum of TK-CPT.

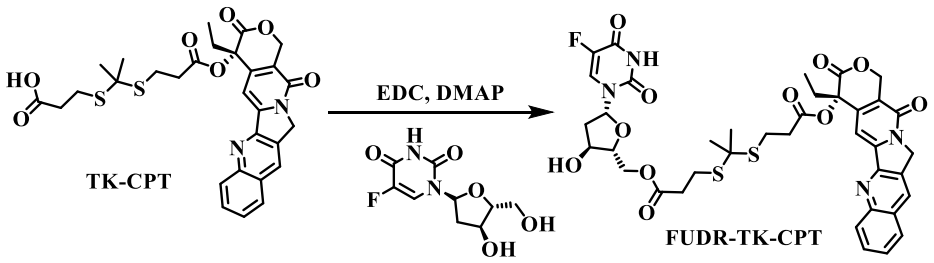

Figure S6. The synthetic route of CPT-TK-FUDR

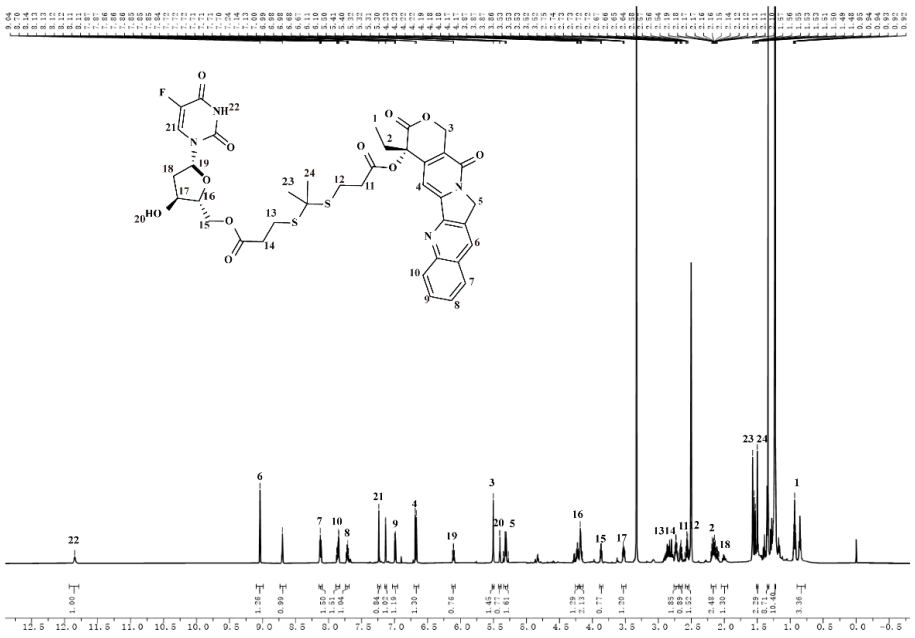

Figure S7. The ^{1}H NMR spectrum of CPT-TK-FUDR in DMSO.

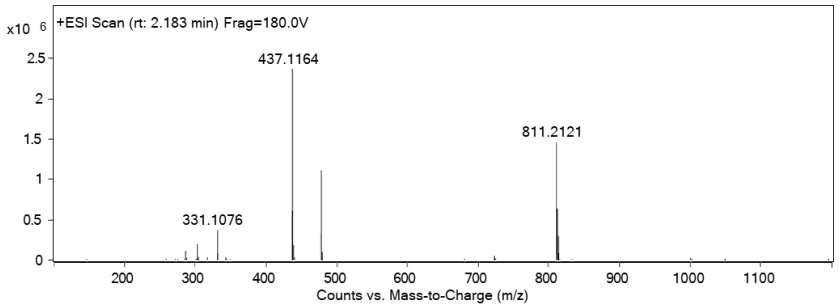

Figure S8. The mass spectrum of CPT-TK-FUDR

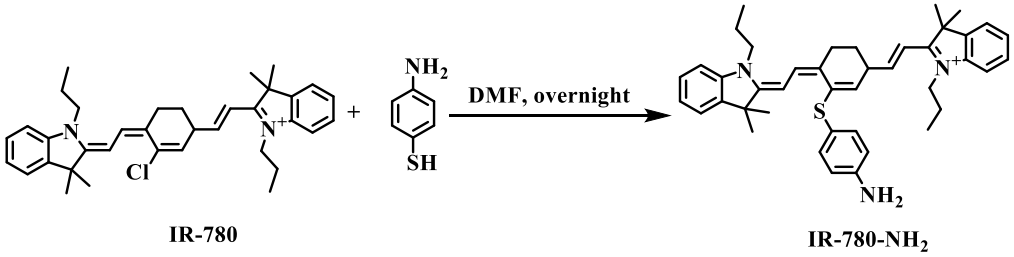

Figure S9. The synthetic route of IR-780-NH_2.

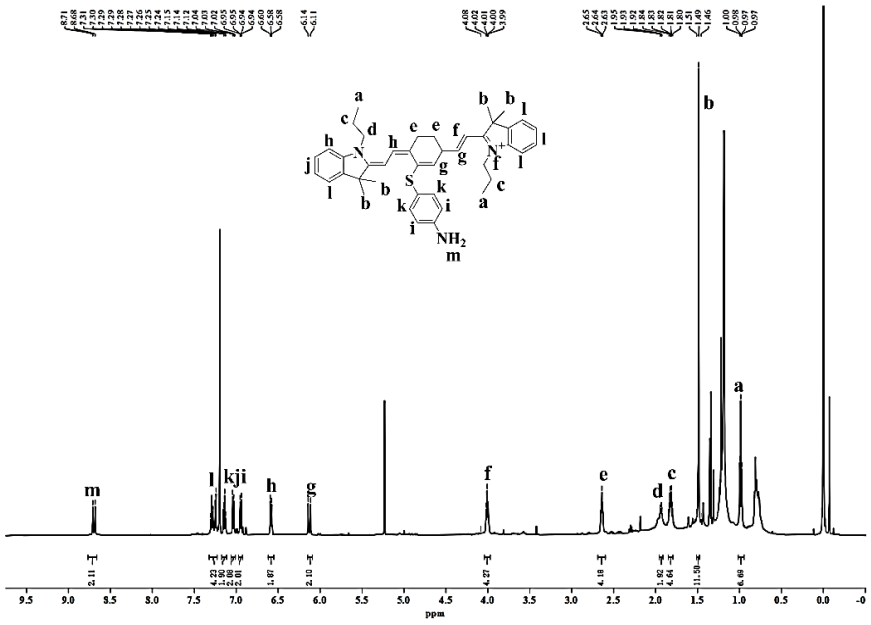

Figure S10. The ^1H NMR spectrum of IR-780-NH_2 in $CDCl_3$.

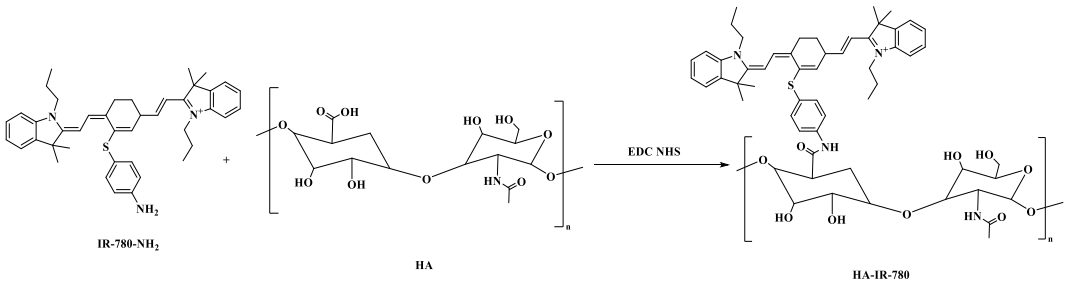

Figure S11. The synthetic route of HA-IR-780.

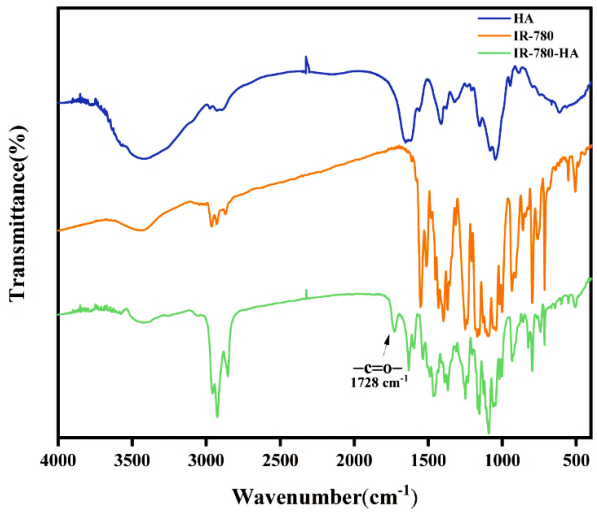

Figure S12. Fourier infrared spectra of HA, IR780 and HA-IR780.

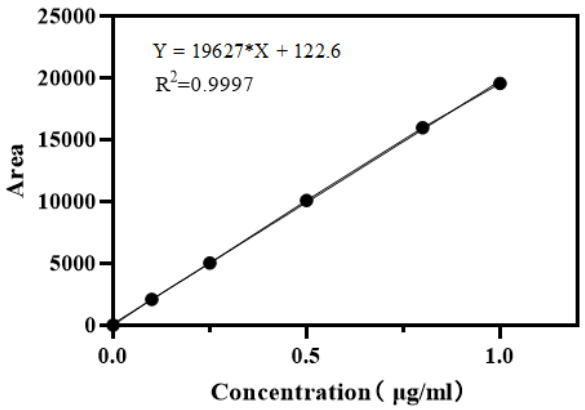

Figure S13. Standard curve of CPT-TK-FUDR

Due to the presence of hydrophilic and hydrophobic parts in $mPEG_{2000}$-DSPE, CTF and HAIR provided hydrophilic and hydrophobicity to form nanoparticles (HAIR/CTF NPs) with $mPEG_{2000}$-DSPE. Therefore, we prepared HAIR/CTF NPs with different drug loadings. The feed mass ratios of mPEG2000-DSPE, CTF, and HAIR included 20:1:(1/5/10/20), 10:1:(1/5/10/20), 5:1:(1/5/10/20), and 1:1:(1/5/10/20), yielding average diameters of 100-200 nm nanoparticles (Figure 2D and S14A) with CTF drug loading efficiency (DLE) of 2.9%, 9.5%, 11.5% and 13.8%, respectively (Figure S14D). The HAIR/CTF NPs prepared with a mass feed ratio of 10:1:5 of $mPEG_{2000}$-DSP to CTF to HAIR had an average diameter of about 146.30 ± 4.94 nm, and the polydispersity index (PDI) of the HAIR/CTF NPs was about 0.106 while the zeta potential was about -11.3 mV (Figure S14B and S14C). Comparing with other formulas, the HAIR/CTF NPs owned a balanced stability, PDI, size and drug loading efficiency with a mass feed ratio of 10:1:5 for $mPEG_{2000}$-DSPE, CTF, and HAIR. Thus, we constructed a stable and high-drug loading NPs in subsequent studies.

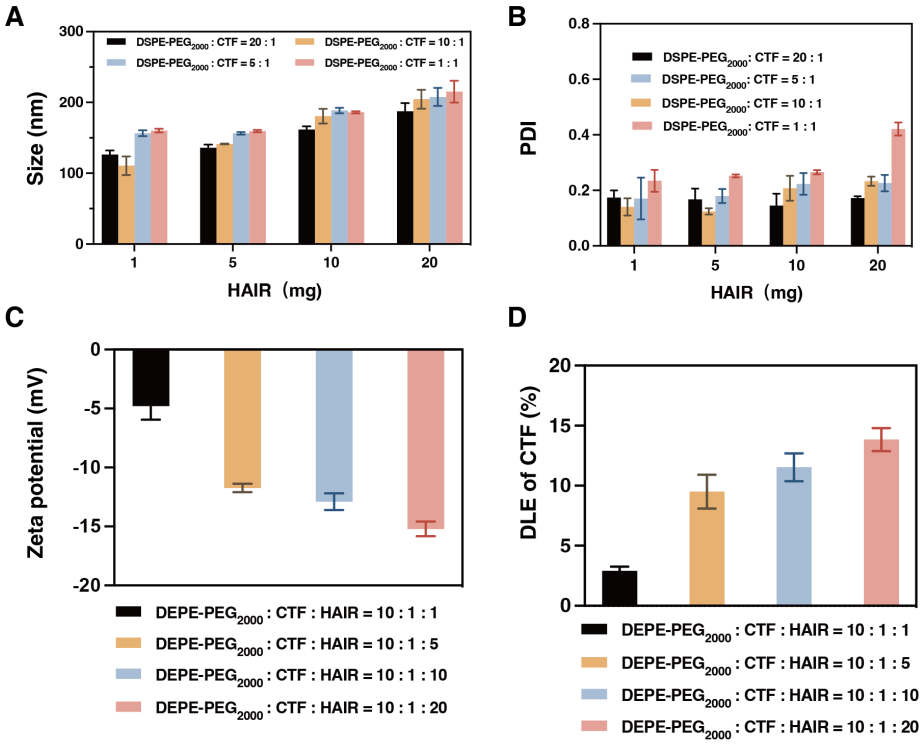

Figure S14. Formula exploration of HAIR/CTF NPs. (A, B, C, D) The size, PDI, zeta-potential and drug loading efficiency of HAIR/CTF NPs by adjusting the ratio of CTF, $mPEG_{2000}$-DSPE and HAIR.

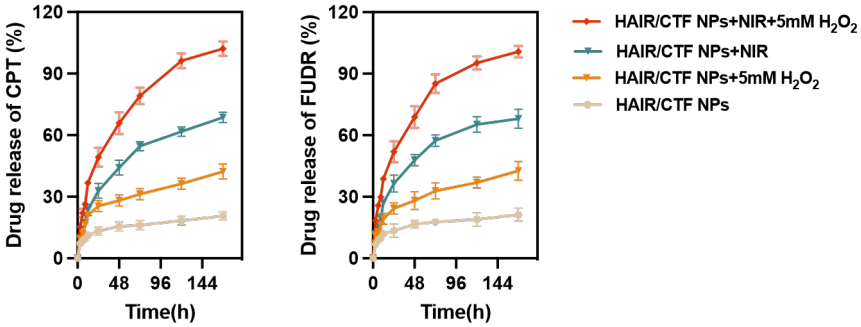

Figure S15. Free drugs release from HAIR/CTF NPs after laser irradiation.

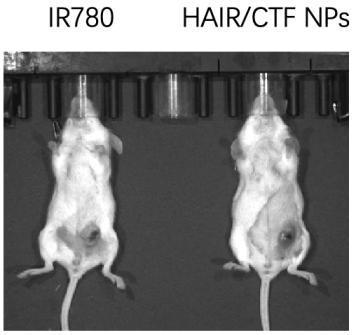

Figure S16. IVIS images of mice before NPs administration (0 h).

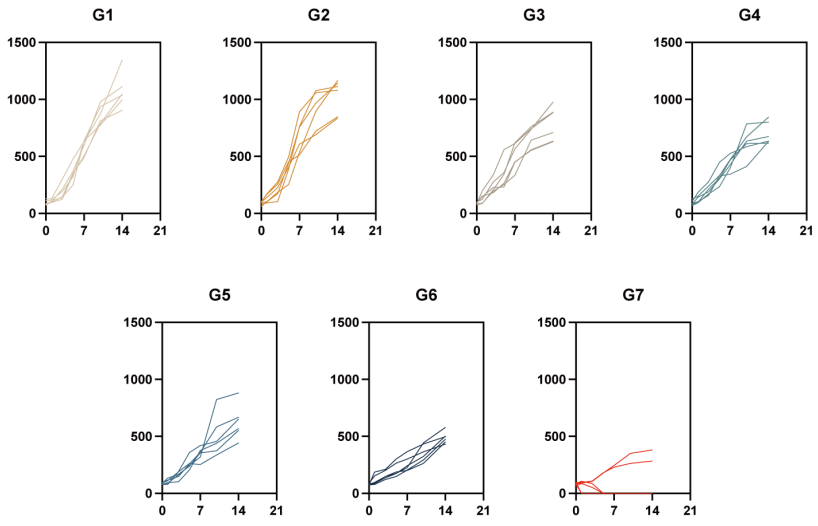

Figure S17. Tumor volume of mice in each group after primary tumor treatments (n=6).

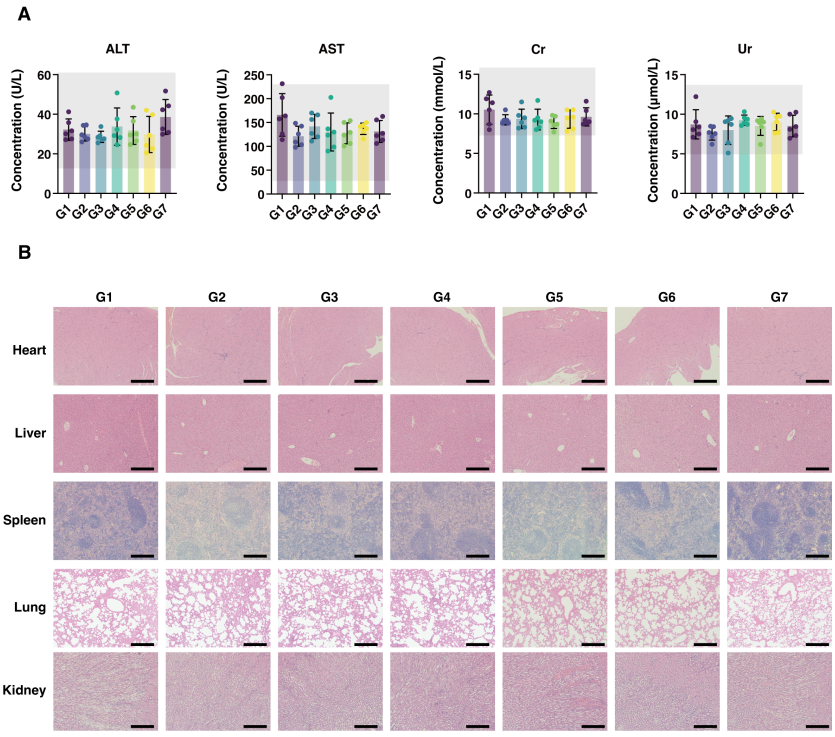

Figure S18. Biosafety evaluation of HAIR/CTF nano-bomb in vivo. (A) Serum levels of ALT, AST, Cr and Ur (n=6). (B) H&E staining images of major organs of mice in each group after different treatments. Scale bar = 200 μm. G1: PBS, G2: PBS+NIR, G3: CTF, G4: HAIR+CTF, G5: HAIR/CTF NPs, G6: HAIR NPs+NIR, G7: HAIR/CTF NPs+NIR. Data = mean ± SD (n = 3).

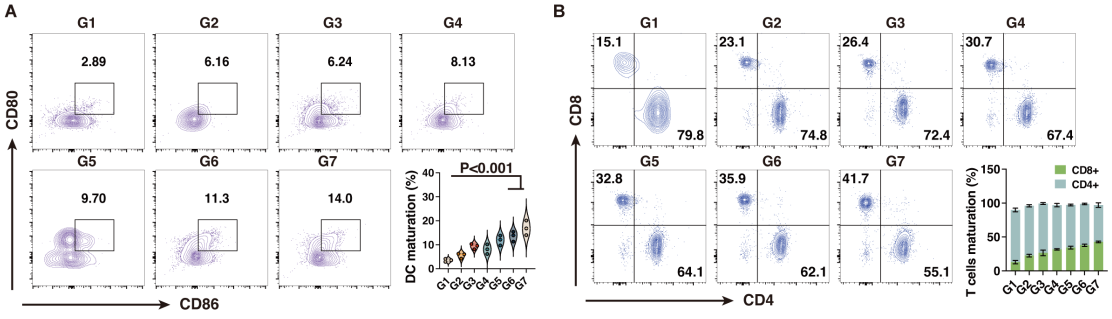

Figure S19. DCs and CTL activation in tumor-draining lymph nodes. (A) DCs maturation analysis in tumor-draining lymph nodes. (B) CTLs activation in tumor-draining lymph nodes. G1: PBS, G2: PBS+NIR, G3: CTF, G4: HAIR+CTF, G5: HAIR/CTF NPs, G6: HAIR NPs+NIR, G7: HAIR/CTF

NPs+NIR. Data = mean ± SD (n = 3). P values were determined by one-way ANOVA followed by Tukey's multiple comparison test.

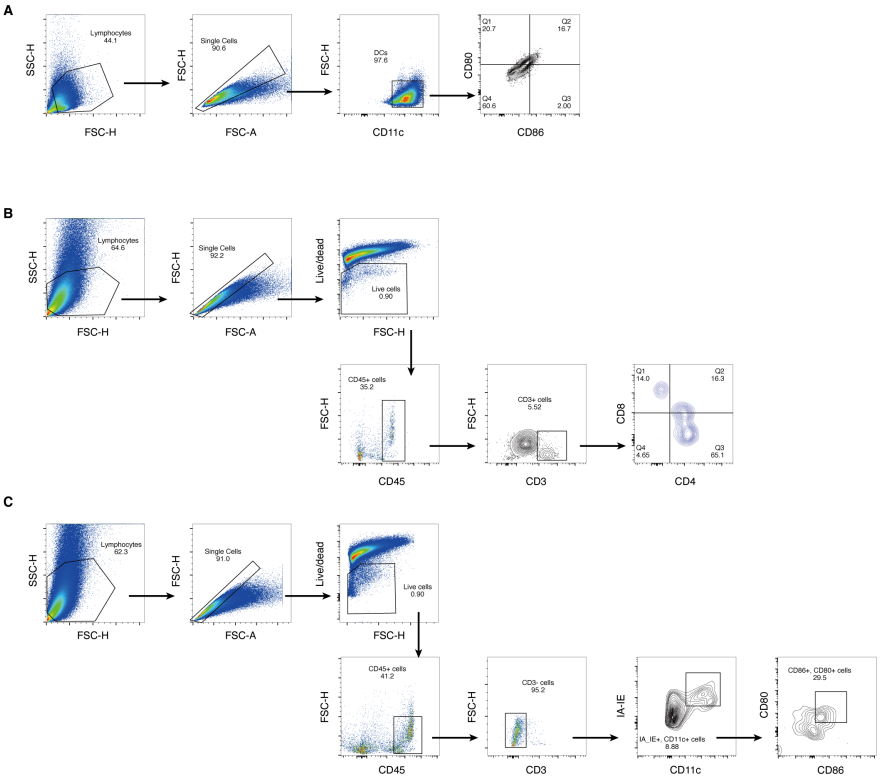

Figure S20. Gating strategy of BMDCs in vitro, DCs in vivo and T cell in vivo. (A) Gating strategy of BMDCs *in vitro*. (B) Gating strategy of DCs in *vivo*. (C) Gating strategy of T cells *in vivo*.